Physica A 475 (2017) 142–154

Contents lists available at ScienceDirect

Physica A

journal homepage: www.elsevier.com/locate/physa

A collision avoidance model for two-pedestrian groups: Considering random avoidance patterns

Zhuping Zhou [a,*], Yifei Cai [a,c], Ruimin Ke [b], Jiwei Yang [a]

[a] Department of Traffic Engineering, Nanjing University of Science and Technology, China
[b] Department of Civil and Environmental Engineering, University of Washington, United States
[c] School of Transportation, Southeast University, China

HIGHLIGHTS

- Velocity obstacle method is applied into modeling the interaction of grouping pedestrians.
- Avoidance model and grouping model are established separately.
- Distance constrained line is developed to describe the relationship between pedestrians.
- Different avoidance patterns can be observed during the simulation.
- The grouping function will decrease the overall velocity of the crowds.

ARTICLE INFO

Article history:
Received 4 August 2016
Available online 7 February 2017

Keywords:
Traffic engineering
Pedestrian grouping behavior
Velocity obstacle
Collision avoidance model

ABSTRACT

Grouping is a common phenomenon in pedestrian crowds and group modeling is still an open challenging problem. When grouping pedestrians avoid each other, different patterns can be observed. Pedestrians can keep close with group members and avoid other groups in cluster. Also, they can avoid other groups separately. Considering this randomness in avoidance patterns, we propose a collision avoidance model for two-pedestrian groups. In our model, the avoidance model is proposed based on velocity obstacle method at first. Then grouping model is established using Distance constrained line (DCL), by transforming DCL into the framework of velocity obstacle, the avoidance model and grouping model are successfully put into one unified calculation structure. Within this structure, an algorithm is developed to solve the problem when solutions of the two models conflict with each other. Two groups of bidirectional pedestrian experiments are designed to verify the model. The accuracy of avoidance behavior and grouping behavior is validated in the microscopic level, while the lane formation phenomenon and fundamental diagrams is validated in the macroscopic level. The experiments results show our model is convincing and has a good expansibility to describe three or more pedestrian groups.

1. Introduction

Pedestrian groups account for large component of urban crowds. According to the statics, 70% of people in a crowd are group pedestrians; the number increases to 85% in some special environments [1]. Although the high ratio group pedestrians

* Correspondence to: Department of Traffic Engineering, Nanjing University of Science and Technology, Nanjing, 210094, China.
E-mail address: jzp19850926@163.com (Z. Zhou).

http://dx.doi.org/10.1016/j.physa.2016.12.041
0378-4371/

count in crowds, almost all microscopic models still focus on interactions between individuals and ignore the influence of grouping pedestrians [2].

When we think about the mechanism of how group pedestrians avoid collisions, we can take an example first. Under the structure of social force model, one pedestrian can be seen as an atom, and the relationship between each pedestrian is like the covalent bond. A pedestrian group is a molecular which contains some atoms, and usually there will be no collision happens because of the van der Waals force. But pedestrian is not atoms, the universal law that every pedestrian must obey does not exists. So rather than impose rules to the pedestrian, a reasonable microscopic model shall respect the randomness of pedestrian and ensure that the model can achieve the necessary microscopic function and macroscopic fundamental diagrams.

We aim to establish a random collision avoidance model for two-pedestrian groups, and prove the model is convincing. Inspired by velocity obstacle method [3], we combine the velocity obstacle with distance constrained line to make sure group pedestrians can keep a reasonable distance with group member and avoid potential collisions.

This paper is structured as follows. In the next section the related work about group modeling is reviewed. In Section 2, we define the variables. Section 3 proposes the avoidance model. In Section 4, the DCL is built and transformed into the calculation framework. Followed, in Section 5, the model solution is then put forward. Section 6 applies the simulation experiments to verify the proposed model. Finally, concluding remarks are provided in Section 7.

2. Related works

Studies of pedestrian behavior have lasted for half a century. Different models have been developed to describe and simulate pedestrian characteristics in realistic walking environment. A well-known model is Helbing's social force model [4] where pedestrians are driven by different force induced by other pedestrians and obstacles. Social force model provides a good thinking to extract a convincing trajectory from the seemly disordered pedestrian behaviors. Zeng extends the model to describe pedestrian behaviors at signalized crosswalk [5]. Fredrik Johansson developed preferred velocity model, preferred position model and adapting preferred position model to describe the waiting pedestrians [6].

Although the SF model is a success, other methods are also applied into modeling pedestrian characteristics under different conditions with different objects, such as evacuation, at bottleneck and at panic, etc. [7–11]. Antonini et al. divided the fan-shaped walking area of a pedestrian into different choice sets and built utility functions to decide which area to walk [12]. Li Xiaona adopted the reciprocal velocity obstacle algorithm to achieve a global path planning, and concluded that in emergency condition, the completion feature would lead to the arching and congestion phenomena [13].

As one of the most well-known methods for agents to avoid collisions with moving obstacles, the velocity obstacle (VO) method does not raise enough attention in pedestrian modeling. Fulgenzi et al. proposed recursive probabilistic velocity obstacles which introduced a type of VO that considers the time interval that guarantees collision avoidance [14]. With a combination of these optimal velocity methods with current pedestrian models, and take grouping behavior into consideration, a new grouping model is possible to be developed.

To achieve a convincing grouping model, an extensive research of grouping behavior and group structure is necessary. Qju and Hu presented a unified framework for modeling the structure aspect of different groups in pedestrian groups and suggest that different group sizes, intra-group structures and inter-group relationships influence the crowd behavior [2]. Ilango et al. studied various factors when pedestrians moving in groups by collecting data in 18 locations in five Indian cities [15]. Xi et al. focused on the spatial pattern, intra-group structure and private space for larger social groups and found that the existence of cellular groups can lead to the multi-pattern of complex social pedestrian groups [16]. Linan Feng developed a framework for charactering hierarchical social groups based on evolving tracklet interaction network which can identify pedestrian dynamic groups from video [17].

Though much works have been conducted, researches especially focus on pedestrian groups and grouping pedestrians are still hard to find. Moussaid added three more patterns including visual, attachment and repulsive force into social force model to illustrate social interaction term, found that crowd dynamics is not only determined by physical constraints induced by other pedestrians and environments, but also by social interactions among individuals [18]. Zanlungo et al. proposed a potential model based on distance and angle to describe the dynamics of the relative motion of two pedestrians socially interacting in a walking group [19]. Tong et al. introduced the group floor field to represent the effect of cohesion force, which preserve the group cohesion and minimize the distances among group members [20]. Ren Gang et al. established a cellular automation model for crossing pedestrians considering the group behaviors, in which the characteristics of pedestrian are described by resistance, direction, empty, conformity and group parameters [21].

3. Variable definition

Suppose that there are n pedestrians walking in a two-dimensional plane (R^2), each pedestrian i ($i = 1, 2, \ldots, n$) has the following properties: a current position (p_i (x_i, y_i)), a current velocity (v_i) and a radius (r_i). These variables are exogenous variables, which can be observed by other pedestrians.

The internal variables are the properties which pedestrian already has, but cannot be observed by other pedestrians. Including:

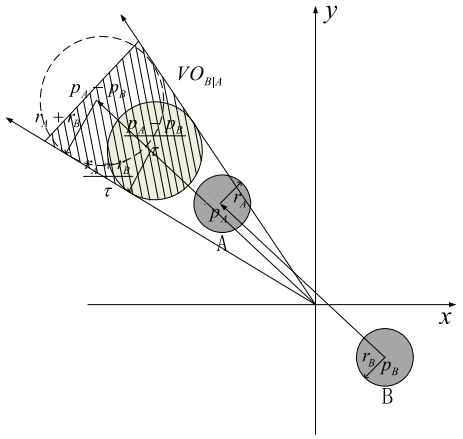

Fig. 1. Velocity obstacle.

(1) Group number (g_i). Pedestrians in the same group share the same number. If a pedestrian is an individual, g_i is set as zero.
(2) Maximum velocity ($v_i^{\max}$) means the maximum walking speed.
(3) Preferred velocity (v_i^{pre}) represents the preference a pedestrian walks towards to the destination at a comfortable velocity. The norm of v_i^{pre} is v_i^* and the direction is e_i^{pre}. v_i^* equals to the average velocity in a free flow and $e_i^{pre} = \frac{p_i - p_d}{|p_i - p_d|}$. $p_d\,(x_d, y_d)$ is the position of destination. Without the interference of other pedestrians, pedestrian i will always walk at the velocity of v_i^{pre}.

4. Avoidance model

4.1. Velocity obstacle

Velocity obstacle has been a successful velocity-based approach for agents to select velocity and avoid collisions with an obstacle moving at a known velocity [22]. And we apply it into our model to describe avoidance behavior. For two individual pedestrians A and B in R^2, if a potential collision between them may happen, both A and B can be seen as an obstacle with velocity to each other. The velocity obstacle for B induced by A is denoted as $VO_{B|A}$.

Let $D\,(p_i, r_i)$ denotes the scope of a circular, r_i and p_i represents the radius and the center of the circular separately:

$$D\,(p_i, r_i) = \{q \mid \|q - p_i\| < r_i\}\,. \tag{1}$$

Then:

$$VO_{B|A} = \{v|\exists t \in [0, \tau] :: tv \in D\,(p_A - p_B, r_A + r_B)\}\,. \tag{2}$$

The velocity obstacle $VO_{B|A}$ can be interpreted as a truncated cone with its apex at the origin and its legs tangent to the circular of radius $r_A + r_B$ centered at $p_A - p_B$. The cone is truncated by an arc of a circular of radius $\frac{r_A + r_B}{\tau}$ centered at $\frac{p_A - p_B}{\tau}$. The amount of truncation depends on the value of τ. The shaded area in Fig. 1 is the velocity obstacle $VO_{B|A}$. When the relative velocity of A and B $v_B - v_A \in VO_{B|A}$, it means that there will be a collision between A and B within time τ, if they keep on their current velocity. Otherwise, A and B are guaranteed to be collision-free. $VO_{A|B}$ and $VO_{B|A}$ are symmetric in the origin.

4.2. Velocity modification

We need to choose a new velocity for both A and B if $v_B - v_A \in VO_{B|A}$. Let μ be the vector from $v_B - v_A$ to the closest point on the boundary of the velocity obstacle $VO_{B|A}$. (See Fig. 2.)

$$\mu = \left(\arg\min_{v \in VO_{B|A}} \|v - (v_B - v_A)\|\right) - (v_B - v_A)\,. \tag{3}$$

The vector of μ is the smallest change of relative velocity $v_B - v_A$ required to avoid collision. Suppose that A and B will share half of the velocity change μ to ensure $v_B - v_A \notin VO_{B|A}$. Assume n is the direction of μ. Hence, the set of $V_{B|A}$ for

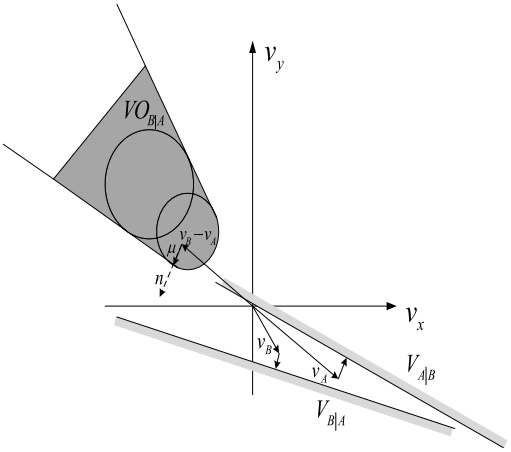

Fig. 2. Velocity choice area of *A* and *B*.

B induced by *A* to choose a new velocity is a half-plane pointing in the direction of n starting at the point $v_B + \frac{1}{2}\mu$. More formally, the $V_{B|A}$ and $V_{A|B}$ is calculated in Eqs. (4) and (5):

$$V_{B|A} = \left\{ v \,\middle|\, \left(v - \left(v_B + \frac{1}{2}\mu \right) \cdot n \right) \geq 0 \right\} \tag{4}$$

$$V_{A|B} = \left\{ v \,\middle|\, \left(v + \left(v_A - \frac{1}{2}\mu \right) \cdot n \right) \geq 0 \right\}. \tag{5}$$

In addition, the results of $V_{B|A}$ and $V_{A|B}$ calculated from $VO_{A|B}$ is the same from $VO_{B|A}$. So, all the following results are calculated from $VO_{B|A}$.

Meanwhile, the new velocity v_B^{new} is constrained by maximum velocity and the willing to keep minimum change to preferred velocity. Let there be k potential avoidance pedestrians around B at time t, then the optimal velocity choice area OVA_B of v_B^{new} is finally denoted as:

$$OVA_B = D\left(0, v_B^{\max}\right) \cap \sum_{i=1}^{k} V_{B|i} \quad i \neq B \tag{6}$$

B will choose the velocity closest to v_B^{pre} from OVA_B:

$$v_B^{new} = \underset{v \in OV_B}{\operatorname{argmin}} \left\| v - v_B^{pre} \right\|. \tag{7}$$

And the new position of *B* at the next time step is:

$$p_B^{new} = p_B + v_B^{new} t. \tag{8}$$

Each pedestrian i performs a continuous cycle of modification with time step t. In each iteration, the pedestrian i infers the optimal velocity choice area OVA_i with respect to each other pedestrian and choose a new velocity which can guarantee a collision-free motion.

5. Grouping model

5.1. Distance constrained line

For pedestrian *A* and *B* with the same group number, let us assume the distance between them is constrained by a force, if the distance r is smaller than normal distance r_0, the force will be attractive, and conversely it will be repulsive. In this paper, the force is named as distance constrained line (DCL). Research (19) provides a simple form of potential function that satisfies the requirements DCL needs.

$$R(r) = \alpha \left(\frac{r_0}{r} + \frac{r}{r_0} \right). \tag{9}$$

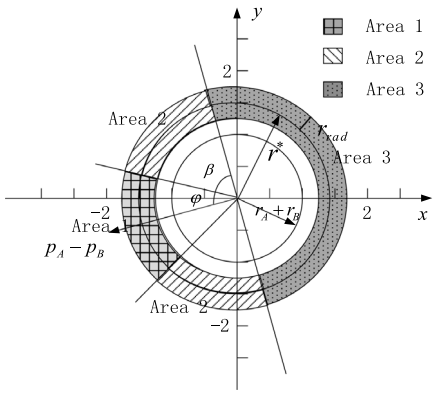

Fig. 3. Grouping displacement constrained area.

Due to the negative gradient of the potential function is the vector of force, then the force for B induced by A is denoted as F_{BA}:

$$F_{BA} = \alpha \left(\frac{r_0}{r^2} - \frac{1}{r_0} \right). \tag{10}$$

Let the norm of relative distance between A and B at time t denote as $L(t)$, then the distance at next time step $L(t+1)$ is:

$$L(t+1) = L(t) + \alpha \left(\frac{r_0}{r^2} - \frac{1}{r_0} \right) t^2. \tag{11}$$

The value range of r is $[r_A + r_B, r_x]$, in this paper, r_x equals to 3 m, when $r > r_x$, or in some special conditions (discussed in Section 6), the DCL is considered disconnected.

An indicator function is added to Eq. (9) to represent the connection and disconnection state of DCL.

$$R(r) = \alpha \left(\frac{r_0}{r} + \frac{r}{r_0} \right) I_D \tag{12}$$

$$I_D = \begin{cases} 1 & g_A = g_B \quad \text{and} \quad r_A + r_B < \sqrt{(x_A - x_B)^2 + (y_A - y_B)^2} < 3 \\ 0 & \text{other.} \end{cases}$$

At the condition when distance r ranges from 3 to 100 m. Suppose A is in front of B. Let the preferred velocity of A stay unchanged, the new preferred velocity v_B^{pre*} of B changes with a new norm of $v_B^{\max}$ and a unchanged direction e_B^{pre}. With a similar destination of A and B, if the time, is long enough, the two grouping pedestrians will always walk into the range within 3 m with Eq. (12) works. Moreover, when the distance is larger than 100 m, A and B are both seen as individuals.

5.2. Grouping displacement constrained area

When DCL is connected, the relative displacement of A and B $p_A - p_B$ at the next time step $t+1$ [1] have to subject to $L(t+1)$. The grouping displacement constrained area $GDCA_{AB}$ for two grouping pedestrians A and B can be interpreted as a ring, the radius of the inner diameter is $L(t+1) - r_{rad}$ and the outer diameter is $L(t+1) + r_{rad}$ (see Fig. 3). For randomness, $r_{rad} \sim N(u, \sigma^2)$. $GDCA_{AB}$ is the area where we select the new relative displacement of A and B at the next time step. To guarantee there is no overlap, if $L(t+1) - r_{rad} < r_A + r_B$, then the radius of the inner diameter changes to $r_A + r_B$ and outer diameter stays unchanged.

$$GDCA_{AB} = \{q \,|\, q \in (D(o, L(t+1) + r_{rad}) - D(o, L(t+1) - r_{rad}))\} \quad L(t+1) - r_{rad} > r_A + r_B \tag{13}$$

$$GDCA_{AB} = \{q \,|\, q \in (D(o, L(t+1) + r_{rad}) - D(o, r_A + r_B))\} \quad L(t+1) - r_{rad} < r_A + r_B. \tag{14}$$

The current relative position is $p_A - p_B$, denoted as $p(t)$. Since the relative displacement change of two grouping pedestrians will not be too far from the current displacement, we add up a limitation into $GDCA_{AB}$. Suppose that in the direction of $p(t) \pm \varphi$ degrees is the area where relative displacement of A and B has the highest possibilities to appear, denoted as Area 1, $GDCA_{AB|1}$. And the area in the direction of $[\varphi, \varphi + \beta]$ and $[-\varphi - \beta, -\varphi]$ with the second possibilities is denoted as Area 2, $GDCA_{AB|2}$. The rest area of the ring is denoted as Area 3, $GDCA_{AB|3}$, the relative displacement will most unlikely appear in this area (see Fig. 3). The relative displacement of A and B will be selected at the order of area 1, 2 and 3.

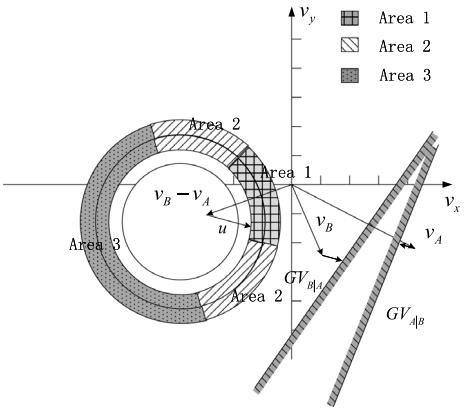

Fig. 4. Grouping velocity constrained area.

5.3. Grouping velocity constrained area

Although the displacement area is constructed, we still cannot select a velocity from displacement constraint. A transformation must be done to combine the grouping model and avoidance model together. Due to:

$$p(t+1) = p(t) + (v_A - v_B)^* t. \tag{15}$$

The relative velocity of A and B should subject to their relative displacement selected from $GDCA_{AB}$. To cope with the calculation form of $v_B - v_A$ in Section 4, the relative velocity considering grouping function is denoted as:

$$(v_B - v_A) = \frac{p(t) - p(t+1)}{t}. \tag{16}$$

For convenience, the time step is set as 1 s. Since $p(t+1)$ is $GDCA_{AB}$, $p(t) = p_A - p_B$. So, the grouping velocity constrained area for two grouping pedestrians A and B, $GVCA_{AB}$ can be seen as a translation of $GVCA_{AB}$ in the vector of $p_B - p_A$, then rotate symmetrically according to the origin (see Fig. 4). In addition, the $GVCA_{AB|1}$ is also translated with $GDCA_{AB}$, and the area 1 of $GVCA_{AB}$ is denoted as $GVCA_{AB|1}$, the same as the area 2 and 3.

When $v_B - v_A \in GVCA_{AB}$, it is unnecessary to modify the relative velocity of A and B, as they are constrained by DCL well. Conversely, the velocity should be modified using the method in Section 4.2. The difference is, the smallest change μ will choose from $GVCA_{AB|1}$ first, then $GVCA_{AB|2}$ and $GVCA_{AB|3}$ at last.

The half-plane where grouping pedestrian B choose a new velocity from induced by grouping pedestrian A is denoted as $GV_{B|A}$. Suppose k potential grouping pedestrians are around B, then the optimal grouping velocity choice area $OGVA_B$ of v_B^{new} is finally denoted as:

$$OGVA_B = D\left(0, v_B^{\max}\right) \cap \sum_{i=1}^{k} GV_{B|i} \quad i \neq B. \tag{17}$$

6. Model solution

To combine the solutions of avoidance model and grouping model together, the total optimal velocity area $TOVA_B$ for v_B^{new} to choose a velocity is:

$$TOVA_B = OVA_B \cap OGVA_B. \tag{18}$$

The next velocity and position of B can be calculated in Eqs. (7) and (8).

Let us assume there are two two-pedestrian groups in R^2, AB and CD, all the individuals is constrained by one grouping half-plane and three avoidance half-plane, the velocity choice sets at time t for B and C is illustrated in Figs. 5a and 5b. To show the results clearly, we ignore the influence of the limitation of maximum velocity.

B should avoid collision with A, C, D and keep distance with A, the $V_{B|A}$, $V_{B|C}$, $V_{B|D}$ and $GV_{B|A}$ form a solvability convex set for B, and v_B^{new} can be easily chosen from the spot area $TOVA_B$. But in Fig. 6, $GV_{C|D}$ cannot constitute a solvability area with other half-plane area, a further consideration is required about the problem.

The reason why it happens is that, for A and B, when they avoid C and D, they do not know whether C and D are grouping, and the current distance between C and D is long enough for AB to pass. But the DCL is working between C and D at time t, and the distance between them in next time step is not enough for AB to go through, that is why $GV_{C|D}$ cannot form a solvability set with the other avoidance half-plane.

Two solutions are listed when $TOV_i = \emptyset$:

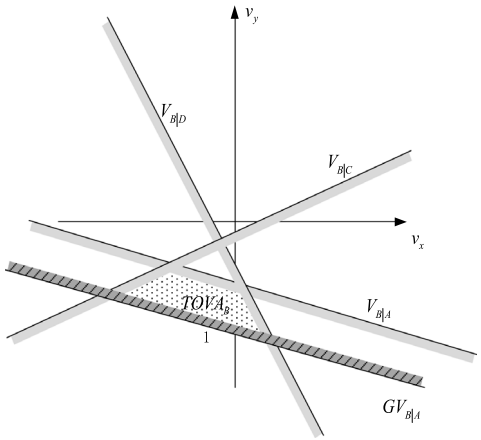

Fig. 5a. *B*'s velocity choice area.

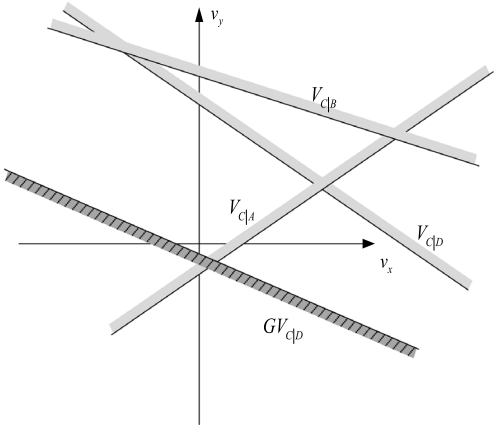

Fig. 5b. *C*'s velocity choice area.

(1) Disconnect the DCL, for the condition in Fig. 6 it means to cancel $GV_{C|D}$.
If the solution 1 is adopted, then:

$$I_D = \begin{cases} 1 & g_C = g_D, \qquad r_C + r_D < \sqrt{(x_C - x_D)^2 + (y_C - y_D)^2} < 3, \qquad TOV_C \neq \emptyset \\ 0 & \text{other.} \end{cases}$$

(2) Replace *C* and *D* with an enveloping circular with radius of $\sqrt{\left(\frac{x_C - x_D}{2}\right)^2 + \left(\frac{y_C - y_D}{2}\right)^2} + \max(r_C, r_D)$ and centered at $\left(\frac{x_C + x_D}{2}, \frac{y_C + y_D}{2}\right)$, for the condition in Fig. 6, the GOV_C does not exist, *CD* are considered as one larger individual for *AB*.

Let the possibility to choose solution 1 become *p*, and the possibility of solution 2 is $1 - p$.

When $TOV_i = \emptyset$, if we select the solution 1, it means v_B^{new} is chosen from OVA_B only, if the solution 2 is selected, the OVA_B will be recalculated and v_B^{new} will be chosen from the new OVA_B^{new}. The whole cycle will continue to perform until all pedestrians get its new velocity.

What is more, in high density, $OVA_B = \emptyset$ may happen as well. In this case, choosing a collision-free velocity cannot be guaranteed, the collision can only be limited to the minimum. Instead, we choose the velocity that minimizes the maximum distance to any of the half-planes induced by the other pedestrians:

$$v_B^{new} = \underset{v \in D(0, v_B^{\max})}{\operatorname{argmin}} \max_{B \neq i} d_{B|i} \quad i = 1, 2, \ldots, n. \tag{19}$$

Algorithm flowchart can be seen in Fig. 6.

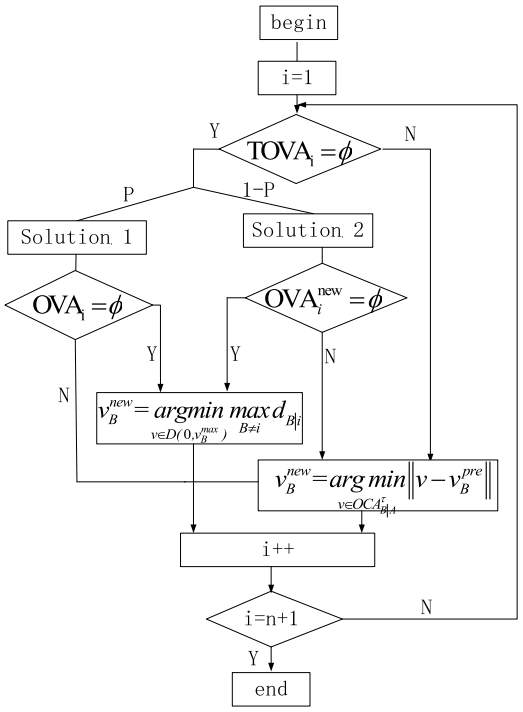

Fig. 6. Algorithm flowchart.

7. Experimental tests and results discussion

The main idea of this section is to prove this model which can achieve the function of keeping a reasonable distance with their group members and avoiding potential collisions. While a reasonable fundamental diagram and aggregate outcomes can be generated.

7.1. Model calibration

In this model, radius of each pedestrian r_i is set as 0.3 m [23], v_i^* is set as 1.34 ± 0.24 m/s [24], maximum velocity $v_i^{\max}$ is 2 m/s, iteration time t is 1 s, and τ is set as 2 s. The parameters μ and σ^2 in normal distribution which r_{rad} subject to is 0.5 and 1, respectively. φ and β is set as 30° and 60° 25. The coefficients still not confirmed are α and r_0 in Eq. (11), and the possibilities p to choose solution 1. First, video data is used to calibrate α and r_0.

At the early stage, model parameters are commonly calibrated by comparing aggregate outcomes and fundamental diagrams [25]. However, it is still unknown whether a microscopic model is able to represent pedestrian walking behavior accurately with a macroscopic calibration method. Recently, some researchers begin to use the maximum log-likelihood estimation method to calibrate microscopic model [26].

The function is set as:

$$f(x) = L(t+1) - L(t) = \alpha\left(\frac{r_0}{r^2} - \frac{1}{r_0}\right)t^2. \tag{20}$$

And the error of the observed and calculated values $f^{obs}(x) - f(x)$ obeys normal distribution:

$$L(\alpha, \sigma) = \frac{1}{\sqrt{2\pi}\sigma}\exp\left[\frac{\left(f^{obs}(x) - f(x)\right)^2}{2\sigma^2}\right]. \tag{21}$$

Let us assume there are n samples and the log-likelihood function is:

$$L = \prod_{i=1}^{n}\frac{1}{\sqrt{2\pi}\sigma}\exp\left[\frac{\left(f^{obs}(x) - f(x)\right)^2}{2\sigma^2}\right]. \tag{22}$$

Table 1
Parameters calibration results.

Variable name	Coefficients estimation	t value	p value
α	1.352	−2.37	0.03
r_0	1.057	2.51	0.04
Log-likelihood values		−350.382	
p^2		0.412	
Sample size		2762	

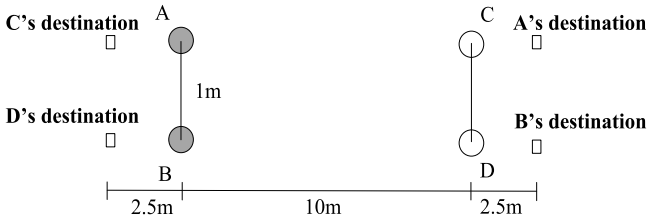

Fig. 7. Test schematic diagram.

Then the calibration results of α and r_0 are obtained which makes Eq. (23) is maximized.

$$\ln L = -\frac{1}{2} n \ln(2\pi) - n \ln(\sigma) - \frac{\sum_{i=1}^{n} \left(f^{obs}(x) - f(x)\right)^2}{2\sigma^2} \tag{23}$$

$$\hat{\alpha} = \arg\max \ln L. \tag{24}$$

The video is recorded at the No. 3 Road of Nanjing University of Science and Technology, May 16, 2016. The experiment section (length = 15 m, width = 3.6 m) is the only way for students to walk to the classrooms. The flow of crowds is large and most pedestrians are grouping pedestrians. Two cameras are set up on the roof of teaching building on both sides of the road; the data was collected in 12:00–13:00 and 15:00–16:00 respectively to eliminate the influence of the density of the crowds. Video is paused at every 0.5 s; the distance change between 235 groups totaling 2762 sets of data is collected. We apply the data set into Biogeme to calibrate the coefficients. Table 1 shows the results.

At 95% of confidence level, t value and p value all demonstrate the coefficients calibration result is credible. The log-likelihood value and goodness of fit p^2 is −350.382 and 0.412, they are all acceptable in practical applications. The estimation value of r_0 is 1.057 which means the average distance between two grouping pedestrians is 1.057 m. The value of α is 1.352, it represents when distance between two grouping pedestrians is smaller than r_0, the relative distance will increase, conversely it decreases, the tendency of the change is consistent with expected results.

7.2. Microscopic phenomenon

The experiment is designed as Fig. 7 to verify that whether the model can achieve expected function, and determine the value of p.

A, B, C, D are four pedestrians in R^2. A and B, C and D are in the same group, the distance of two groups is 10 m. Each pedestrian wants to arrive at the destination with straight-line distance of 12.5 m. Four pedestrians start at the same time, and the simulation stops until all pedestrian arrive at their own destination. The experiments is conducted repeatedly at 1000 times, for each pedestrian, the distance with his group member, the distance with the closest pedestrian who is not in the same group are count every 0.5 s at the frame velocity of 16 frame/s. Once the condition of relative distance between any two pedestrians is less than 0.6 m occurs, it can be considered as a conflict.

7.2.1. Avoidance behavior

First, the p value is determined in this experiment. Because the different values of p decides the avoid strategy when grouping model and avoidance model conflict with each other, it will change the pattern of avoidance, so the optimal value of p is decided by the avoidance pattern. Suppose the value of p is 0, 0.1, 0.2… 1. And repeat the experiments above 1000 times for every assumed p value, then compare the avoidance pattern of experiments with actual 233 sets of collision avoidance between two-pedestrian groups collected in video. What is more, the average distance between each pedestrian with its closest pedestrian is considered as an auxiliary decision variable. The results are shown in Table 2.

When $p = i$, let the ratio of pattern 1, 2, 3 and the average closest distance denote as p_i^1, p_i^2, p_i^3 and l_i, the value of video is considered as p_r^1, p_r^2, p_r^3 and l_r. Then the optimal value of p is:

$$p = \arg\min \left[\sum_{k=1}^{3} (p_i^k - p_i^k)^2 + (l_i - l_r)^2 \right]. \tag{25}$$

Table 2
Avoidance patterns.

p value	Pattern 1		Pattern 2		Pattern 3		Average closest distance (m)
	Number	Ratio	Number	Ratio	Number	Ratio	
0	82	8.20%	15	1.50%	903	90.30%	1.053
0.1	85	8.50%	58	5.80%	857	85.70%	1.051
0.2	86	8.60%	91	9.10%	823	82.30%	1.049
0.3	112	11.20%	92	9.20%	796	79.60%	1.051
0.4	108	10.80%	127	12.70%	765	76.50%	1.048
0.5	95	9.50%	164	16.40%	741	74.10%	1.046
0.6	100	10.00%	167	16.70%	733	73.30%	1.047
0.7	134	13.40%	146	14.60%	720	72.00%	1.049
0.8	116	11.60%	172	17.20%	712	71.20%	1.047
0.9	145	14.50%	152	15.20%	703	70.30%	1.050
1	161	16.10%	140	14.00%	699	69.90%	1.051
Video	20	8.58%	25	10.73%	188	80.68%	1.076

The calculation results show that $p = 0.2$ is the most suitable value. We can conclude from the Table 2 that the value of p decides the number of pattern 3. The smaller the p is, the more number of pattern 3 generates. We do not find a close relationship between p and the average closest distance, the fluctuation of the distance in all 10 000 times of experiments is not obvious. The value of the distance is slightly smaller than video data that is because the initial distance is set as 1 m. During the whole progress, no distance between every pedestrian is smaller than 0.65 m, we are glad to find that the collision avoidance performs so well in low density, and it proves that avoidance behavior of this model is credible.

7.2.2. Grouping behavior

To confirm the grouping function in this model, we select representative trajectories of 4 pedestrians A, B, C, D in different three patterns when $p = 0.2$. Each position point is selected at every 0.5 s in Fig. 8(a)–(c). The line between grouping pedestrians is represented as DCL, when it is black it means the DCL is connected and the red means disconnected.

As shown in Fig. 11, it is obvious that members of two groups always keep a reasonable distance with each other. The DCL is connected in the whole process and drives group pedestrians to avoid opposite pedestrians together. In Fig. 9, for avoiding CD, the DCL between A and B is disconnected at the time when $TOVA_A$ and $TOVA_B = \emptyset$, while reconnect at the time when the solution is nonempty. Similarly, in Fig. 10, DCL of both AB and CD is disconnected to ensure no collision happens, all four pedestrians are seen as individuals and they choose to walk through the mid gap between each other. There is no doubt that many factors can lead to different avoidance patterns of these four pedestrians. Taking pattern 3 for example, a possibility that the DCL between AB and CD are both disconnected, and these four individuals still walk together to complete the avoidance, and that is the randomness reflects in this model. After all, it still can be observed from three trajectories that the relationship between connection status of DCL and avoidance patterns is obvious, which means the grouping function is effective.

7.3. Macroscopic phenomenon

After verifying the microscopic characteristics, the microscopic phenomenon generated by this model should be compared with practical situation as well. Normally, it contains comparing with aggregate outcomes and well-known phenomena such as lane formation and clogging. We design a bidirectional pedestrian experiment to verify our model, the experiment is a rectangular region with length 15 m from $x = 0$ m to $x = 15$ m and width 4 m from $y = 0$ m to $y = 4$ m. The flow is input at the rate of $5p$/m s at both side of the rectangular in the area of $x = 0, 15$ and $y = [1, 3]$. Ratio of grouping pedestrians and individuals is 3:2. The simulation runs through a warm-up period of 100 s, and data is extracted after the simulation is stable. We use the Voronoi diagram to calculate velocity and density in measurement area [27], as the Voronoi cells capture more precisely the effectively occupied space by pedestrians at the boundaries than dividing the measurement area into same pieces of areas (see Fig. 9).

For pedestrian i, each pedestrian in the measurement region will be divided into a unique Voronoi cell. Let us assume that: the area of measurement region A is S, the number of Voronoi cell is n, and velocity of pedestrian is v_i. Then, the density and velocity distribution of the space p_{xy} and v_{xy} is:

$$p_{xy} = \frac{1}{S} \quad \text{and} \quad v_{xy} = v_i \quad \text{if } (x, y) \in A. \tag{26}$$

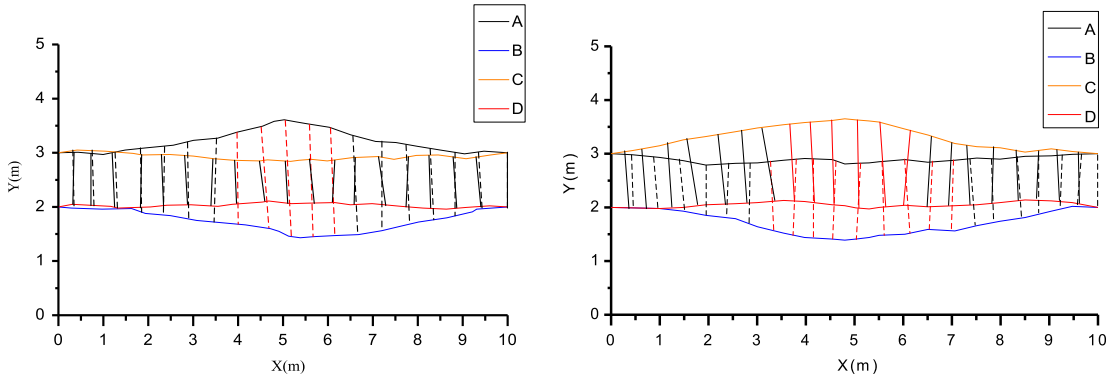

(a) Trajectory of pattern 1.

(b) Trajectory of pattern 2.

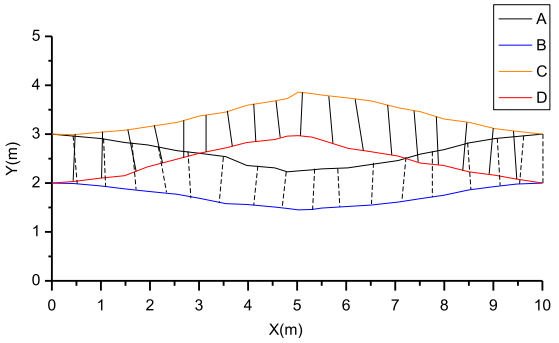

(c) Trajectory of pattern 3.

Fig. 8. Trajectory of different patterns. (For interpretation of the references to color in this figure legend, the reader is referred to the web version of this article.)

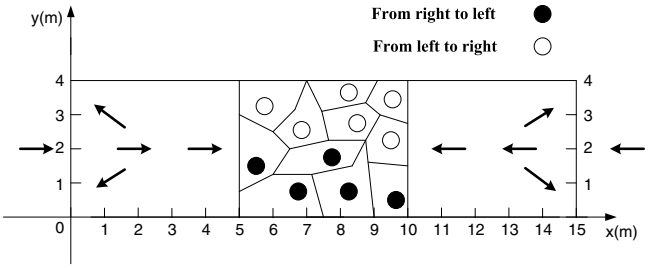

Fig. 9. Bidirectional experiments.

The Voronoi density and velocity for the measurement area is defined as Eq. (27):

$$p_A = \frac{\iint p_{xy} d_x d_y}{S} \tag{27}$$

$$v_A = \frac{\iint v_{xy} d_x d_y}{S}. \tag{28}$$

7.3.1. Lane formation

For bidirectional pedestrian flow, the most obvious phenomenon can be observed is lane formation. We calculate the velocity and density in every 1 m^2 at time $t = 10$ s (160 frame) of the bidirectional experiment for verification (see Figs. 10a, 10b).

In Fig. 10b, an obvious lane formation can be observed. Pedestrians walk from left to right form a crowd that move rightwards in $y = 1 - 3$ m, and pedestrians walk from right to left form two flows moving bypass. We do not find a clear lane formation in the density distribution diagram, but we find that the central area is the most concentrated area, and the velocity in this area is disturbed seriously by opposite flows, there is a significant reduction of velocity in this area.

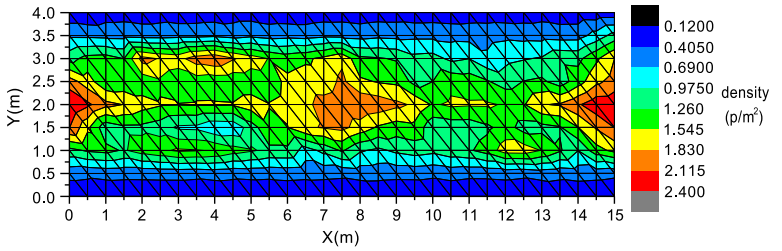

Fig. 10a. Density distribution diagram.

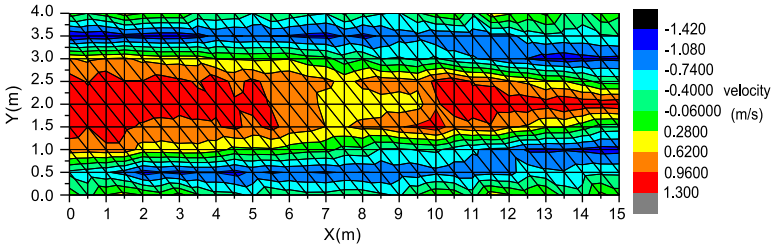

Fig. 10b. Velocity distribution diagram.

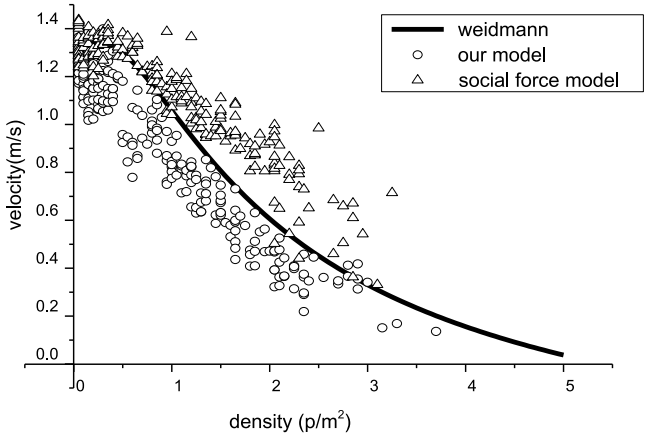

Fig. 11. Density-flow fundamental diagram.

Because in theory building we do not focus on the lane formation phenomenon, after a careful check of the simulation, we find that when $p = 0.2$, most of the pedestrians take the avoidance in pattern 3, and there is a high possibility that the velocity modify results of the pedestrians behind is same as pedestrians in front, that is why a so obvious lane formation phenomenon generate, which prove the accuracy of our model in microscopic level.

7.3.2. Comparison of fundamental diagram

The social force model is the most widely known as a microscopic simulation model of pedestrian dynamics on arbitrary topologies. We compare the fundamental diagram of social force model, our model and weidmann curve to confirm the aggregate phenomenon of our model is convincing. The areas with $x = 5-10$ m and $y = 0-4$ m are chosen as measurement area. Because the area of the pedestrian in our model is 0.283 m^2, so the highest density is 3.53 p/m^2. Since there is no grouping function in social force model, the input of this model is all set as individuals. The velocity and density is count at every 160 frames, the results of density-flow fundamental diagrams can be seen in Fig. 11.

The trend of our model and social force model is consistent with weidmann curve, the density increases while the velocity decreases. When the density is less than 1 p/m^2, no obvious difference is found in these two models, but when the density increases, the grouping function becomes notable, the overall velocity of our model becomes smaller than social force model. Although we cannot prove one model is better than the other by comparing the fundamental diagrams, since the outcomes of our model is consistent with the widely acceptable model and the survey data so well, we can still say that our model is convincing.

8. Conclusions

In this paper, a new method is applied to establish the collision avoidance model for two-pedestrian groups. This model can ensure two grouping pedestrians keep a reasonable distance and avoid collision with other pedestrians, when there is a conflict between grouping model and avoidance model, pedestrians can also complete the avoidance motion as realistic as possible. We design two groups of experiments to verify the model in microscopic and macroscopic level. The conclusions are as below:

1. The value of p influences the number of avoidance pattern 3. The smaller the p is, the more number of pattern 3 generates.
2. The connection of DCL has a direct influence to the trajectory of grouping pedestrians and the avoidance patterns.
3. In high density situation, the velocity modification results of pedestrians in front will influence the pedestrians behind.
4. The grouping function will decrease the overall velocity of the crowds.
5. At the premise of considering randomness, the collision avoidance model is convincing in both microscopic and macroscopic level.

In the next stage of work, we will focus on how DCL works in three and more group pedestrians. DCL works well when handling the problem of two-pedestrian groups, but when it comes to multi-pedestrian groups; it is hard to decide how a pedestrian is connected with other pedestrians in one group. Zanlungo used the way of potential function (15), but it also constrains the flexibility of multi-pedestrian groups, we think that if we improve the DCL continuously, the more reasonable grouping pedestrian model is possible to be established.

Acknowledgments

This research is supported by the National Natural Science Foundation of China (51308298), China Postdoctoral Science Foundation funded project (2014M561653), National Key Research and Development Program: key projects of international scientific and technological innovation cooperation between governments (2016YFE0108000), and the Fundamental Research Funds for the Central Universities (30916011335).

References

[1] Francesco Zanlungo, Drazem Brscic, Takayuki Kanda, Pedestrian group behavior analysis under different density conditions, Trans. Res. Proc. 2 (2) (2014) 149–158.
[2] Fasheng Qju, Xiaolin Hu, Modeling group structures in pedestrian crowd simulation, 18 (2010) 190–205.
[3] Z.P. Zhou, Y.S. Liu, W. Wang, Y. Zhang, Multinomial logit model of pedestrian crossing behaviors at signalized intersections, Discrete Dyn. Nat. Soc. (2013) 1–8.
[4] Dirk Helbing, Peter Molnar, Social force model for pedestrian dynamics, Phys. Rev. E 51 (5) (1995) 51–56.
[5] Weiliang Zeng, Application of social force model to pedestrian behavior analysis at signalized crosswalk, Transp. Res. C 40 (2014) 143–159.
[6] Fredrik Johansson, Anders Peterson, Andreas Tapani, Waiting pedestrians in the social force model, Physica A 419 (2015) 95–107.
[7] Baibing Li, A model of pedestrian intended waiting times for street crossing at signalized intersections, Transp. Res. B 51 (2013) 17–28.
[8] Sun Ze, Jia Bin, Li. Xingang, The study of the interference between pedestrians and vehicles based on cellular automaton model, Acta Phys. Sin. 61 (10) (2012) 1–8.
[9] Ming Tang, Hongfei Jia, Bin Ran, et al., Analysis of the pedestrian arching at bottleneck based on a bypassing behavior model, Physica A 453 (1) (2016) 242–258.
[10] Serge P. Hoogendoorn, W. Daamen, Pedestrian behavior at bottlenecks, Transp. Sci. 39 (2) (2005) 147–159.
[11] Dong Liyun, Chen Li, Duan Xiaoyin, Modeling and simulation of pedestrian evacuation from a single-exit classroom based on experimental features, Acta Phys. Sin. 64 (22) (2015) 1–10.
[12] Gianluca Antonini, Michel Bierlaire, Mats Weber, Discrete choice models of pedestrian walking behavior, Transp. Res. B 40 (2006) 667–687.
[13] Xiaona Li, Wenhu Qin, A crowd behavior model based on reciprocal velocity obstacle algorithm, in: 2012 International Workshop on Information and Electronics Engineering, 2012.
[14] C. Fulgenzi, A. Spalanzani, C. Laugier, Dynamic obstacle avoidance in uncertain environment combining PVOs and occupancy grid, in: 2007 IEEE International Conference on Robotics and Automation, IEEE, 2007.
[15] T. Ilango, Rajat Rastogi, Satish Chandra, Behavior and perception of pedestrians walking in groups, in: Transportation Research Board 2011 Annual Meeting, 2011.
[16] Jiaan Xi, Xiaolei Zou, Zhuo Chen, Multi-pattern of complex social pedestrian groups, in: The Conference on Pedestrian and Evacuation Dynamics, 2014.
[17] Linan Feng, Bir Bhanu, Understanding dynamic social grouping behaviors of pedestrians, IEEE J. Sel. Top. Signal Process. 9 (2) (2015) 317–329.
[18] M. Moussaid, N. Perozo, S. Garnier, et al., The walking behavior of pedestrian social groups and its impact on crowd dynamics, PLoS One 5 (4) (2010) e10047.
[19] Francesco Zanlungo, Tetsushi Ikeda, Takayuki Kanda, Potential for the dynamics of pedestrians in a socially interacting group, Phys. Rev. E 89 (5) (2014) 1–18.
[20] Tong Weiping, Chen Lin, An extended floor field model based on cellular automata for pedestrian and group behavior, Syst. Eng.-Theory Pract. 34 (9) (2014) 2387–2391.
[21] Ren Gang, Ding Chenzi, L.U. Lili, Model and simulation of group pedestrian flow on a crosswalk based on cellular automaton, J. Transp. Syst. Eng. Inf. Technol. 14 (2) (2014) 45–50.
[22] P. Fiorini, Z. Shiller, Motion planning in dynamic environments using Velocity Obstacles, Int. J. Robot. Res. 17 (7) (1998) 760–772.
[23] J. Fruin, Pedestrian and Planning Design, Metropolitan Association of Urban Designer and Environmental Planners Inc., New York, 1971.
[24] A. Seyfried, A. Portz, A. Schadschneider, Phase coexistence in congested states of pedestrian dynamics, Cell. Autom. (2010).
[25] W. Daamen, S.P. Hoogendoorn, Calibration of pedestrian simulation model for emergency doors for different pedestrian types, Transp. Res. Rec. 2316 (1) (2012) 69–75.
[26] Gunnar Flotterod, Gerogor Lammel, Bidirectional pedestrian fundamental diagram, Transp. Res. B 72 (2015) 194–212.
[27] J. Zhang, W. Klingsch, A. Schadschneider, A. Seyfried, Transitions in pedestrian fundamental diagrams of straight corridors and t-junctions, J. Stat. Mech. (06) (2011) P06004.